PROGRESS IN COLOR, COLORANTS AND COATINGS

available online @ www.pccc.icrc.ac.ir

Progress in Color Colorants Coating 18 (2025), 201-218

Ministry of Science, Research and Technology
Institute for Color Science & Technology

Fabrication of Solar-Driven New Composite Heterostructure $CoWO_4$/NCW Photo catalysts for Enhanced Adsorption/Photo Degradation Activity of Organic Pollutants

A. A. Hassan [1,2,3*], I. Kareem Shakir[3]

[1.] Department of Chemical, Engineering, University of Muthanna, P.O. Box: 1550, Muthanna, Iraq.
[2.] Department of Petroleum Engineering, Al-Ayen University, P.O. Box: 64141, Thi-Qar, Iraq.
[3.] Department of Chemical Engineering, University of Baghdad, P.O. Box: 1417, Baghdad, Iraq.

ARTICLE INFO

Article history:
Received: 09 July 2024
Final Revised: 15 Nov 2024
Accepted: 30 Nov 2024
Available online: 31 Dec 2024

Keywords:
Water treatment
Textile
Cellulose
Tungstate
Composite

ABSTRACT

In this work, abundant natural and industrial materials were used in concert to create a new nanocomposite made of Nano cellulose (NCW) hydrolyzed by nitric acid and cobalt tungstate ($CoWO_4$) prepared by precipitation methods from sodium tungstate and cobalt chloride. The result was a cost-effective nanocomposite used as an adsorbent and photo-degradation with exceptional organic pollutants (OP) in refinery wastewater (RWW). This composite exhibited outstanding mechanical stability and eliminated organic pollutants (OP) by oxidation and adsorbent. All materials were comprehensively characterized through XRD, FTIR, DRS, TGA, BET, EDX, XRD, and FE-SEM analyses. A comparison was made between the nanocomposite's UV and solar light performance, considering factors like temperature, pH, time, dose, and so on. The best conditions were identified: pH levels of 8-9, time of 120 minutes, temperature of 70 °C, and dose of 1.0 g. Upon applying these optimized conditions to RWW samples, the high removal ratios were achieved: 97.4, 90.3, 64.2, and 49 % for $CoWO_4$/NCW, NCW, NaOH/CW, and CW respectively. These findings underscore the composite's potential as an economical and efficient biosorbent for OP elimination, alongside its effectiveness in solar-assisted degradation processes. Prog. Color Colorants Coat. 18 (2025), 201-218© Institute for Color Science and Technology.

1. Introduction

Huge amounts of wastewater are discharged annually into the environment from different domestic and industrial activities around the world [1]. Domestic wastewater contains several types of biodegradable contaminants that differ in their types and concentrations depending on humans' demands [2], and contains biodegradable and non-biodegradable pollutants such as oil pollutants, COD, BOD, TOC, high salinity, and toxic metals, wastewaters discharged from oil-refining activities vary from one phase to another owing to the difference in the kind of crude oil treated [3]. Therefore, wastewater should be treated before being discharged into the soil or the aquatic systems by using practical treatment methods [4]. Nanocellulose has garnered significant interest due to its biodegradability, distinctive chemical and physical traits, diverse origins, and broad utility [5]. It can be synthesized from cellulose obtained from natural cellulose fibers, which can exist in either fibrous or crystalline forms [6]. Previous studies have indicated that nanocellulose possesses a surface abundant in reactive hydroxyl groups. This feature enables facile modification of nanocellulose, thereby enhancing its applicability and value across various domains [7]. Cotton, a linear

*Corresponding author: * ali.alkhafaji@mu.edu.iq
https://doi.org/10.30509/pccc.2024.167338.1308

cellulose polymer, comprises repeating units of cellobiose, each composed of two glucose units. Thanks to advancements in nanotechnology, nanocellulose extracted from cotton waste has emerged as a notable development [8], Due to its affordability, bio-compatibility, renewability, exceptional reactivity, and desirable physical attributes [9]. Nanocellulose offers distinct advantages over cellulose microcrystalline, including higher crystallinity, improved tensile strength, increased hydrophilicity, and a supramolecular structure [10]. These attributes render nanocellulose preferable for assembling and advancing polymer composites. Researchers have merged nanocellulose with conventional metal oxide semiconductors, creating a hybrid composite [11]. These hybrid composites provide additional active sites due to their increased surface area and expanded wavelength response range in visible light. This enhancement facilitates improved metal ion adsorption onto the catalyst's surface, thereby enhancing the efficiency of photocatalytic degradation [12]. Photocatalytic and film composites offer an advantage by circumventing the challenges associated with recovering and removing metal oxide suspensions in water post-photocatalytic organic degradation [13]. Transition metal tungstate, especially those with the wolframite structure, have shown promising properties for various applications due to their unique electronic and structural characteristics [14]. Using them for photocatalytic degradation of organic substances is a clever utilization of their potential. Transition metals similar to manganese (Mn), cobalt (Co), iron (Fe), copper (Cu), nickel (Ni), lead (Pb), zinc (Zn), and infrequent earth elements have distinct electronic shapes and activities of catalytic, which could offer diverse options for enhancing the photocatalytic methods. Cobalt tungstate ($CoWO_4$), a renowned p-type semi-conductor, finds numerous requests, counting its use as pigment additives [15]. The preparation of $CoWO_4$ materials has garnered increasing attention because of their significant requests [16]. This method uses solar energy to degrade damaging organic and inorganic materials present in oily wastewater. Particularly, its non-toxic nature, ambient temperature process, and low cost have elevated its significance [17]. While TiO_2 is widely utilized as a photocatalytic material, its limited activation under visible light hampers its efficiency [18]. Titanium dioxide has emerged as a visible light photocatalyst, but its effectiveness is hindered by the rapid recombination of photogenerated electron/hole pairs. To address this issue, coupling with other semiconductor materials is essential to form heterogeneous structures like $CoWO_4$/NCW. This enhances the photocatalytic effectiveness through restricting electron/hole recombination [19].

In this work prepared new composite $CoWO_4$/NCW from Combining $CoWO_4$ nanoparticles with NCW prepared from CW through nitric acid hydrolysis could with unique properties and applications. The prepared $CoWO_4$/NCW, was employed for the adsorption and solar catalytic degradation of OP in RWW under solar irradiation. Composite dose, pH, oxidation time and temperature were examined to enhance the adsorption /solar oxidation processes.

2. Experimental

2.1. Materials and analysis test

The wastewater contaminated with organic contaminants was gotten from oilfields refinery. Refinery wastewater was conserved at (6 °C) to be treated through the treatment. The wastewater properties is listed in Table 1. All materials used in this work were of analytical grade and purification. Cotton waste was composed from couture workshops and exposed to cutting and shredding procedures. H_2SO_4, NaCl, CCl_4, H_2O_2, NaOH, $Na_2WO_4.2H_2O$), and $CoCl_2.6H_2O$ used for wet chemical methods. All experiments were test, 0.15 g of NaCl is added to 35 mL of RWW in a separating funnel. Sodium chloride is used to disrupt the emulsion of organic pollutants, helping to separate the organic phase more effectively. After adding sodium chloride, 4 mL of carbon tetrachloride is added to the separating funnel. RWW in the separating funnel is vigorously shaken for 2 minutes. This agitation helps to ensure thorough mixing of the phases and facilitates the extraction of organic content into the carbon tetrachloride phase. After that, the solution is allowed to stand for 20 minutes. The UV-1800 spectrophotometer is used to measure the absorbance and from the standard curve find the concentration of organic in ppm.

The organic elimination efficacy (Eq. 1) was assessed:

$$Y_{OC}=\frac{C_o-C_t}{C_o}\times 100\% \quad (1)$$

Where C_o and C_t are the initial and final concentration in RWW, respectively.

Table 1: Properties of refinery wastewater.

Limits	Values	Limits	Values
Organic concentration	164 ppm	Solution oxygen content	0.035 mg/L
Turbidity	25.2 NTU	TSS	21.3 ppm
pH	6.89	Viscosity	1.023 m Pa S^{-1}
Conductivity	452631 µs/cm	Density	977.3 Kg/m^3

2.2. Nano cellulose preparation

The CW was cleaned via cold and hot water correspondingly until a constant coloring was visually experiential in the water. Next to the washing steps, cotton waste was impregnated in a 5 % sodium hydroxide and stirred incessantly with the same of [20]. In an oven set for one day, the CW was dried at 70 °C to finish the washing procedure. After that, the impregnated in a solution with hydrogen peroxide and acetic acid (2/7 %). 15/20 mL of concentrated nitric acid and distilled water were combined in a vessel used for NCW synthesis. The mixture was heated to 40 °C while being continuously stirred for three hours to guarantee complete mixing. As shown in Figure 1, the ensuing liquid was repeatedly rinsed with water until a pH of neutral was reached.

2.3. Preparation of $CoWO_4$/ NCW

The wet-chemically made composite, containing $CoWO_4$ nanoparticles, is supported on nanocellulose. The temperature of solution was adjusted by [19] with some modification. To achieve complete mixing, 0.5 g of Nano cellulose are ultrasonically sonicated for 25 minutes in 100 milliliters of deionized (DI) water. The solution is then stirred for an additional 30 minutes. Cobalt chloride (0.225 g) is added to the Nano particles suspension.

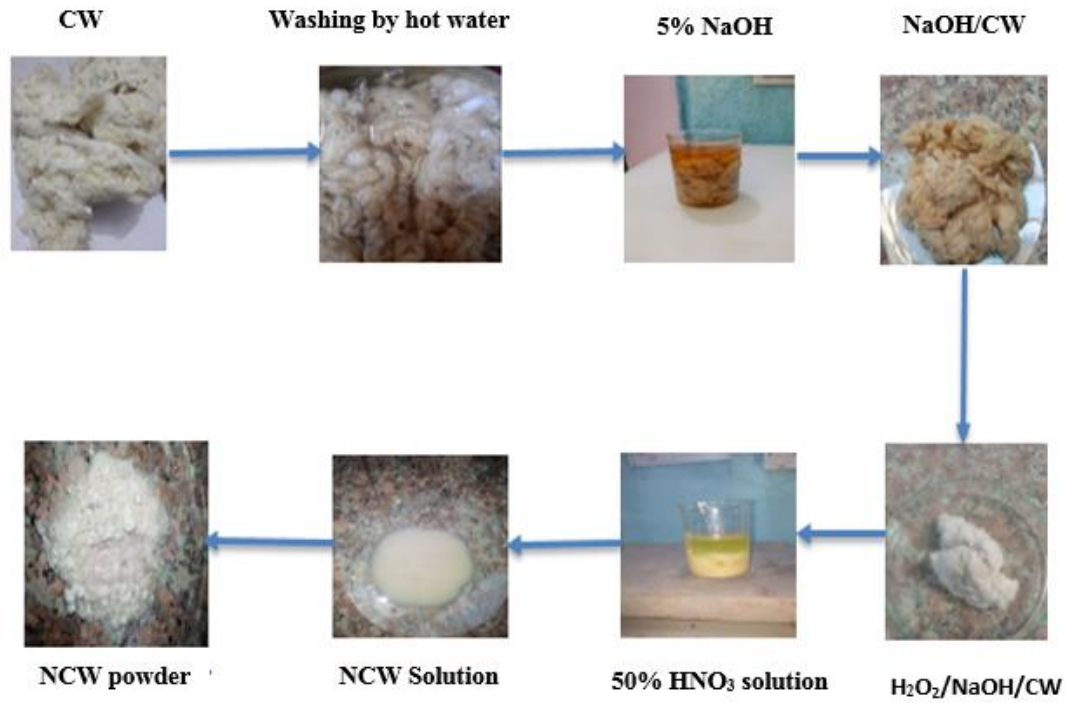

Figure 1: Preparation of nano cellulose.

Cobalt chloride synthesis as a precursor for the new composite cobalt component. By dissolving 0.18 g of Na_2WO_4 in DI water, a sodium tungstate solution is created. Stirring continuously, 25 mL of the sodium tungstate solution is gradually added to the cobalt chloride-containing NCW suspension. Furthermore, 25 minutes after the injection of the sodium tungstate solution, ultra-sonication is accomplished once more. This stage facilitates the creation of the nanocomposite and guarantees complete mixing for 3 h. The hybrid nanocomposite is separated from the liquid solution as presented in Figure 2. Lastly, the purified nano-composite is dried overnight at 60 °C to remove any remaining solvent and obtain the final product used in work as adsorbent and solar degradation.

2.4. Characterization

Analytical methods were used to measure the structural, morphological, thermal, and other properties of the new composites. FTIR analysis was performed with the attenuated total reflectance technique, yielding results in the 4000-400 cm^{-1} range. The composite adsorbent's surface morphology was examined using a FE-SEM. The Nano cellulose preparation and their existence in the $CoWO_4$/NCW composites were demonstrated to be confirmed by XRD analysis. TGA was carried out using a Q-500 from TA instruments. The thermal stability and decomposition performance of the samples were assessed by heating them at a rate of 10 °C/min in an inert atmosphere. To work the elemental configuration of the composite materials, FE-SEM was combined with EDX, a chemical microanalysis tool. Using UV-Visible diffuse reflectance spectroscopy, the novel semiconductor composite's energy band gap was being measured. Using a Thermo Analyzer/USA, the Brunauer, Emmett, and Teller approach was used to measure the surface area and pore volume.

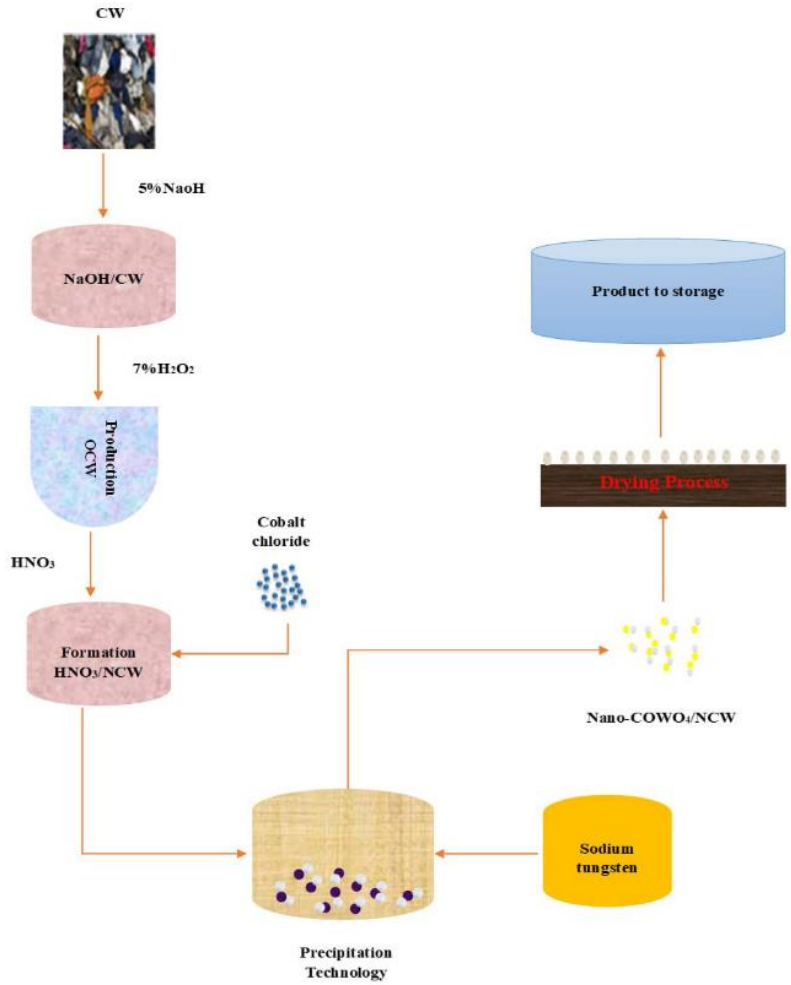

Figure 2: $CoWO_4$/NCW preparation.

2.5. Batch procedure

The solar/adsorption degradation studies were conducted in a batch reactor, which is a kind of vessel designed to carry out work in a regulated situation. A magnetic stirrer was employed to ensure uniform mixing of the RWW within the nanocomposite in the reactor. Before the addition of the composite, the pH of the RWW was adjusted using dilute basic or acid solutions. The pH adjustment is vital as it can affect the adsorption capacity and competence of the treatment process. Figure 3 illustrates the setup used for the refinery wastewater treatment under a sun source. It may include the adsorbent composite used for OP removal and the solar light where the solar degradation process takes place.

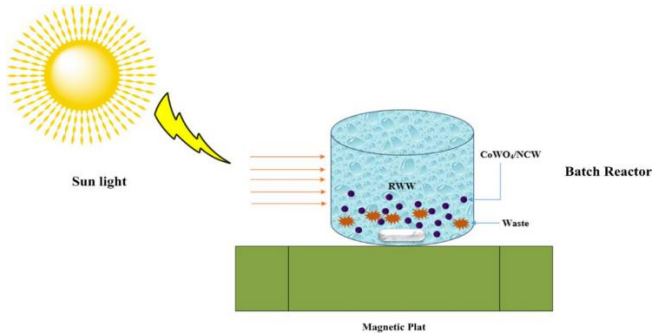

Figure 3: Solar degradation for RWW.

2.6. Experimental design

This work recognized the use of the $CoWO_4$/NCW composite to optimize inexperienced conditions for RWW mineralization and contaminants. This purpose was being pursued by the Box-Bingham design (BBD) method in conjunction with Response Surface Methodology. The software Minitab-17 was utilized for statistical analysis, graphical depiction, and experimental design of oxidation time (X_1) ,pH (X_2), dosage (X_3), and Temperature (X_4), were the independent factors taken into consideration.

3. Results and Discussion

3.1. Characteristics of $CoWO_4$/NCW

FT-IR spectroscopy shows that the oxidation reaction significantly affects the structure of CW, NCW, and $CoWO_4$/NCW. The region from 3000 to 3600 cm^{-1} in the FT-IR spectroscopy analysis shown in Figure 4 corresponds to –OH stretching vibrations, which are mostly associated to the amount of hydroxyl groups in CW and other composites. The relative intensities in this range drop subsequent treatment of oxidation, signifying a notable decrease in the amount of hydroxyl groups current. The mechanical qualities of treated cotton waste are lost as a consequence of this decrease in the partial breakage of hydrogen bond structures in CW. The experiential upsurge in the intensity of the band at around 1716 cm^{-1}, consistent with C=O stretching vibrations, the changes in the chemical composition of the CW with increasing oxidation levels. Exactly, this change is accredited to the creation or introduction of aldehyde and carboxylate groups throughout the oxidation Nano cellulose process [21]. The XRD analysis as presented in Figure 5, the characteristic peaks of the NCW sample specify a sodality structure, consistent with standard peaks of NCW. The absence of substantial changes to the XRD planes proposes that the particles are efficiently prepared and well-formed, representative high crystallinity, Sharp peaks are experiential at $2\theta = 22.59$, representative the typical pattern of type I cellulose for NCW. For $CoWO_4$, an amorphous structure is experiential, with typical diffraction peaks alike to those of a $CoWO_4$ sample organized by [22]. The lack of important changes in the XRD patterns specifies that the particles prepared, counting the $CoWO_4$ catalyst, maintain their crystalline structure finished the oxidation of NCW. The synthesized material's crystalline nature is further confirmed by the identification of distinctive diffraction peaks [23]. Next the production of binary and/or triple nanocomposites, some of the individual component diffraction peaks vanish, which is symptomatic of the formation of crystalline structure. The prominent peaks of each component are still discernible or just slightly shift from their initial locations, but the nanocomposites still have some of the key components' properties [24]. The particles display a uniform, polyhedral, almost hexagonal or spherical nanocrystal line structure. The grains are arranged in sizes ranging from 27 to 63 nm, with an average size of 50 nm from the FE-SEM picture in Figure 6. The average particle size of NCW nanoparticles is 40 nm, and they range in size from 15 to 65 nm. Figure 7 shows a 90 nm-size of prepared new composite, which is the result of partial dispersion of $CoWO_4$ on NCW and shows a homogenous distribution of nanoparticles. The morphology of cellulose is in line with earlier reports published by Simayee et al., offering

confirmation and consistency to the characterization procedure [25]. The Cobalt tungstate is successfully encapsulated within NCW to form composite, as shown in Figures 6J, 6K, and 6L. This encapsulation causes the size of the nanoparticle to grow to around 90 nm. Here's a summary of the characterization results. EDX analysis was conducted to assess the purity of NCW and $CoWO_4$/NCW presented in Figure 8 for NCW and nanocomposite. The analysis revealed the presence of Co, W, C, and O elements in the samples, as listed in Table 2. No impurity peaks were experiential, representative high sample purity and confirming the attendance of the intended elements analysis was utilized to determine the optical characteristics of the prepared catalyst and assess its ability to produce electron-hole pairs during the solar degradation process [26]. The thermogravimetric curves of the nanomaterial produced by hydrolyzing nitric acid from CW are shown in Figure 9. The main cause of the early weight loss noticed up to 105 °C is the evaporation of water from the CW. NCW and $CoWO_4$ are reported to have beginning degradation temperatures of 287 and 316 °C, respectively. The formation of new composite through steam explosion and mild acid conduct enhances the thermal stability of NCW, perhaps because of partial destruction of the crystalline area. This a change in the molecular structure, by way of observed in the TGA curves, which is related to thermal decomposition [27]. Moreover, the thermal transitions in this temperature range are related with the onset of thermal degradation of cellulose, including rearrangement of molecular chains, cleavage of glycosidic bonds, and intermolecular cross-linking. Using a BET device, the prepared NCW sample's surface area and pore volume were analyzed. It is found that the surface area derived from the current investigation is 16.4 m^2/g. It's important to note that this measurement of BET surface area is greater than that which Pandi et al. reported, suggesting that there may have been changes in sample preparation, untried setup, or logical approaches between works. The BET surface area measurements were 11.423 and 0.5642 m^2/g for 5 and 30 % of cobalt tungstate on Nano cellulose [28]. In the manner shown in Figure 10. The homogeneous distribution of the nanoparticles on the cellulose surface and their larger surface area could enhanced the competence of photo absorption. The loading of $CoWO_4$ NPs on the prepared Nano cellulose may cause Clogging of a portion of pores which result in a reduction of surface area and pore volume. Among them, CoWO4/NCW shows BET surface area and relatively high nitrogen sorption. The pores in the higher surface area usually are very small as shown in Figure 11.

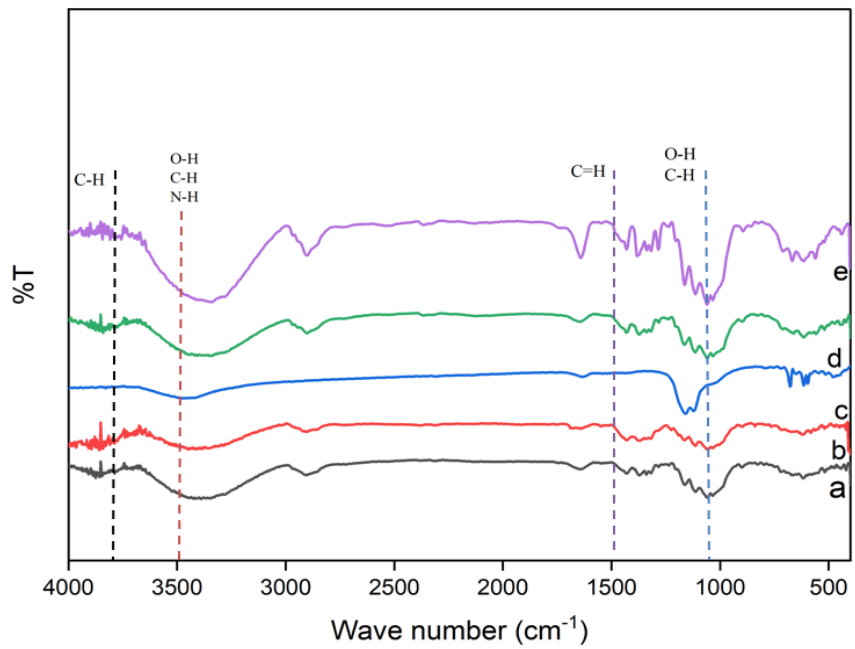

Figure 4: FTIR of a) Cotton waste, b) NaOH/CW, c) OCW, d) NCW and e) $CoWO_4$/NCW.

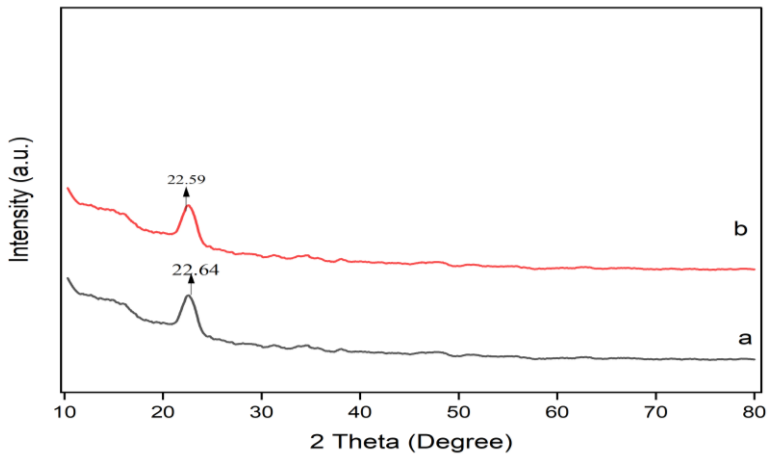

Figure 5: XRD of a) nano cellulose and b) prepared composite of $CoWO_4$/NCW.

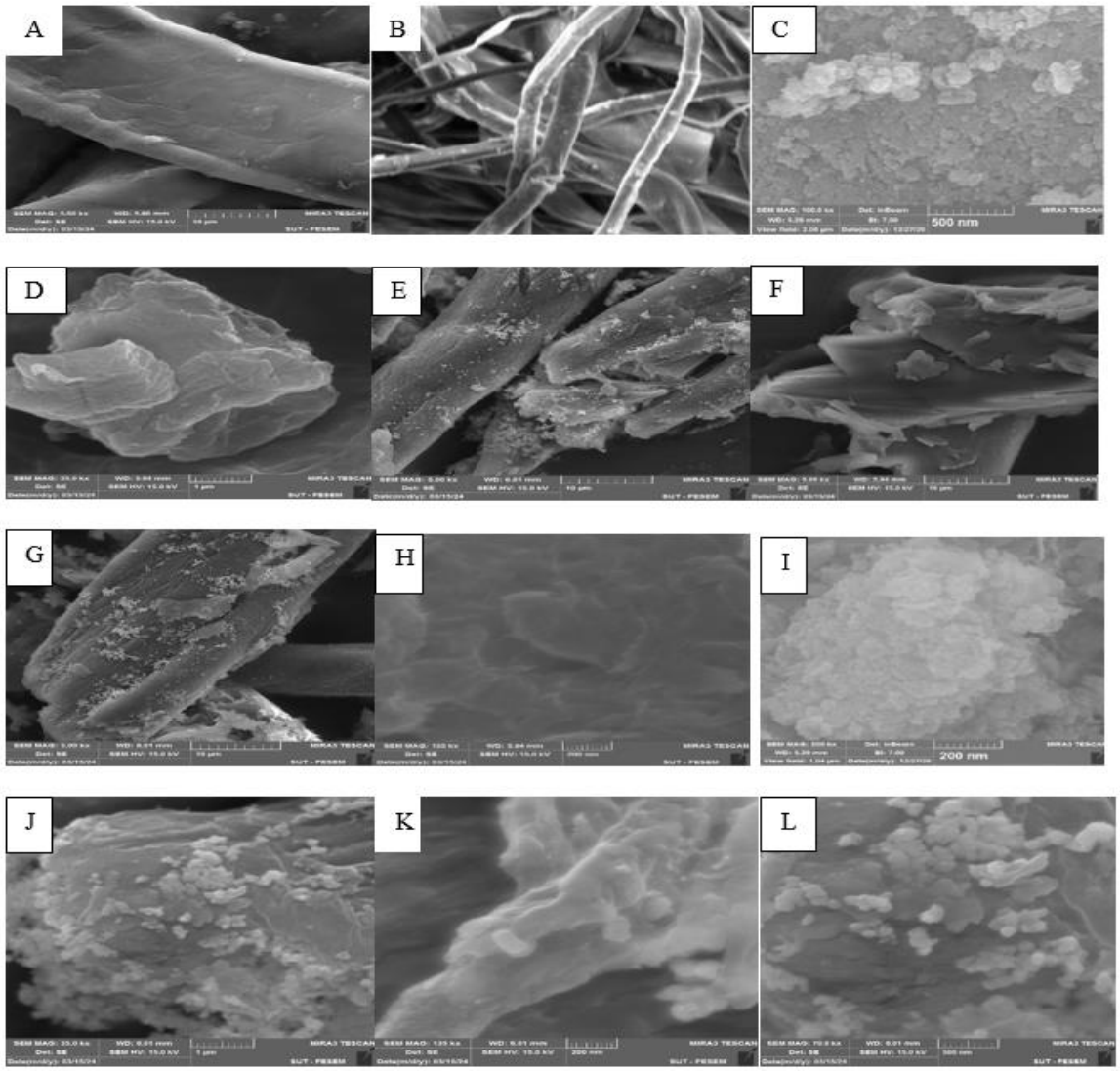

Figure 6: A) CW at 10 µm, B) CW at 25 µm, C) $CoWO_4$ at 500 nm particles, D) Nano cellulose at 1 µm, E) $CoWO_4$/NCW at 1 µm, F) Nano cellulose at 10 µm, G) $CoWO_4$/NCW at 10 µm,(H) Nano cellulose at 200 nm, (I) $CoWO_4$ at 200 nm, J) $CoWO_4$/NCW at 1 µm, K) $CoWO_4$/NCW at 200 nm and L)$CoWO_4$/NCW at 500 nm.

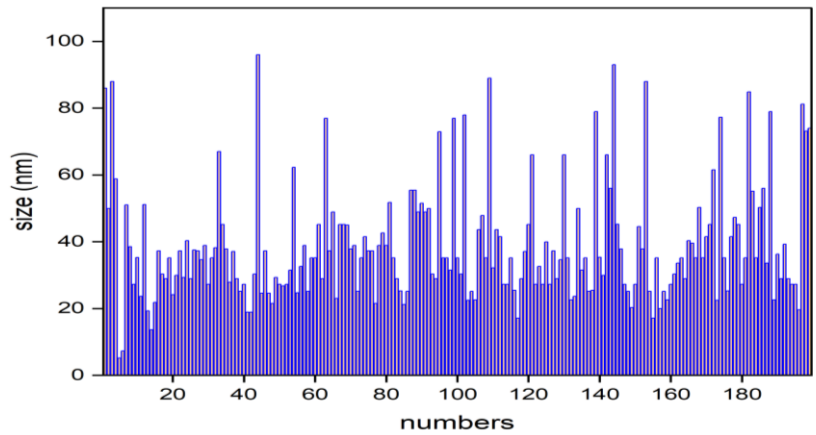

Figure 7: Diameter distribution of prepared composite.

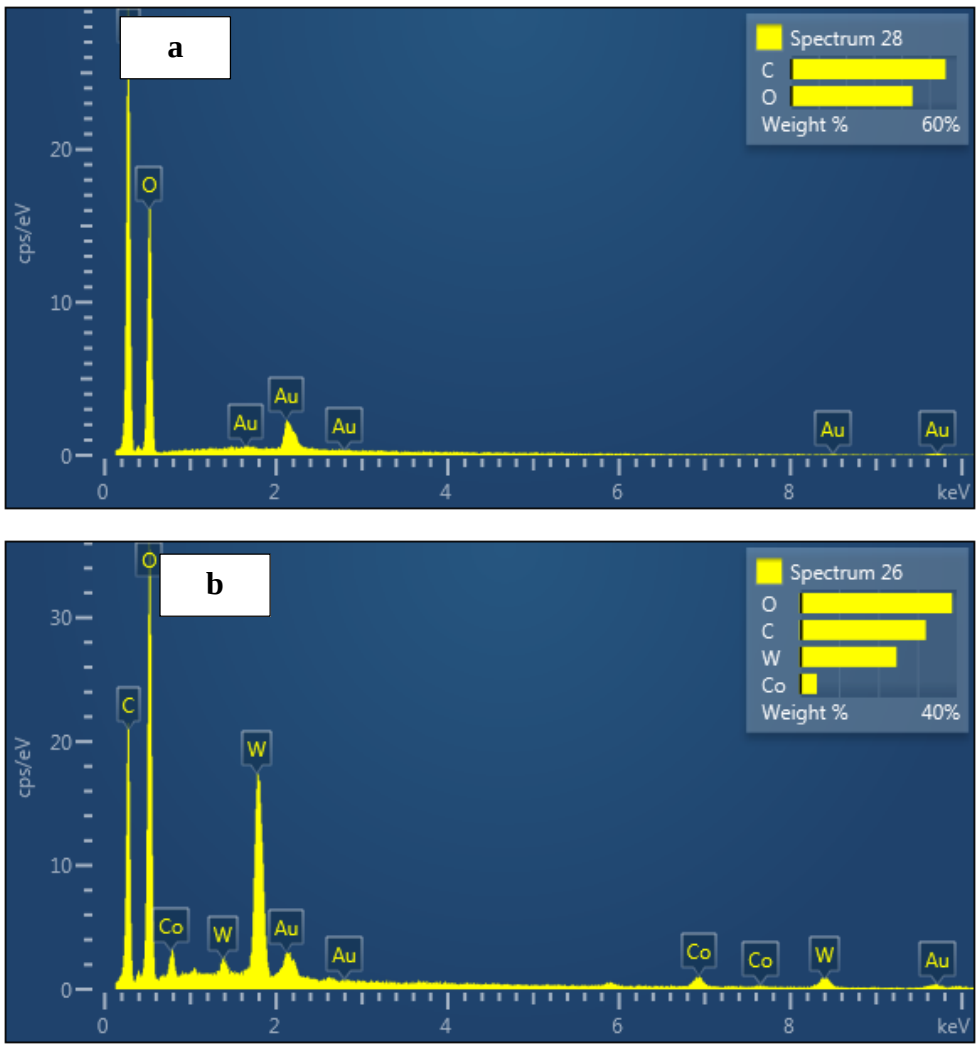

Figure 8: EDX of a) Nano cellulose and b) prepared composite.

Table 2: EDX for NCW and $CoWO_4$/NCW.

Element	Nano cellulose		$CoWO_4$/NCW	
	Wt. %	Atomic %	Wt. %	Atomic %
C	55.97	62.87	32.11	50.37
O	44.03	41.81	38.80	45.69
Co	-	-	4.42	1.41
W	-	-	24.66	2.53
Total:	100.00	100.00	100.00	100.00

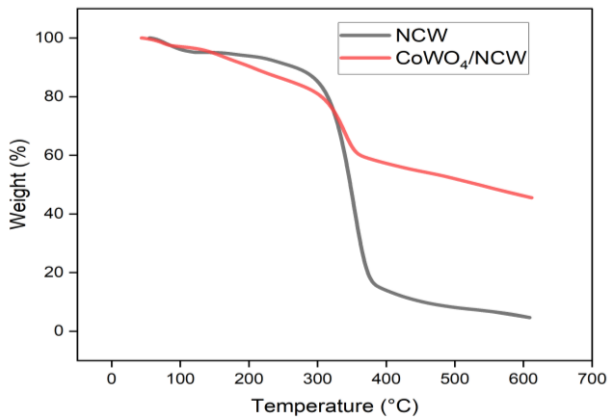

Figure 9: TGA for Nano cellulose and $CoWO_4$/NCW.

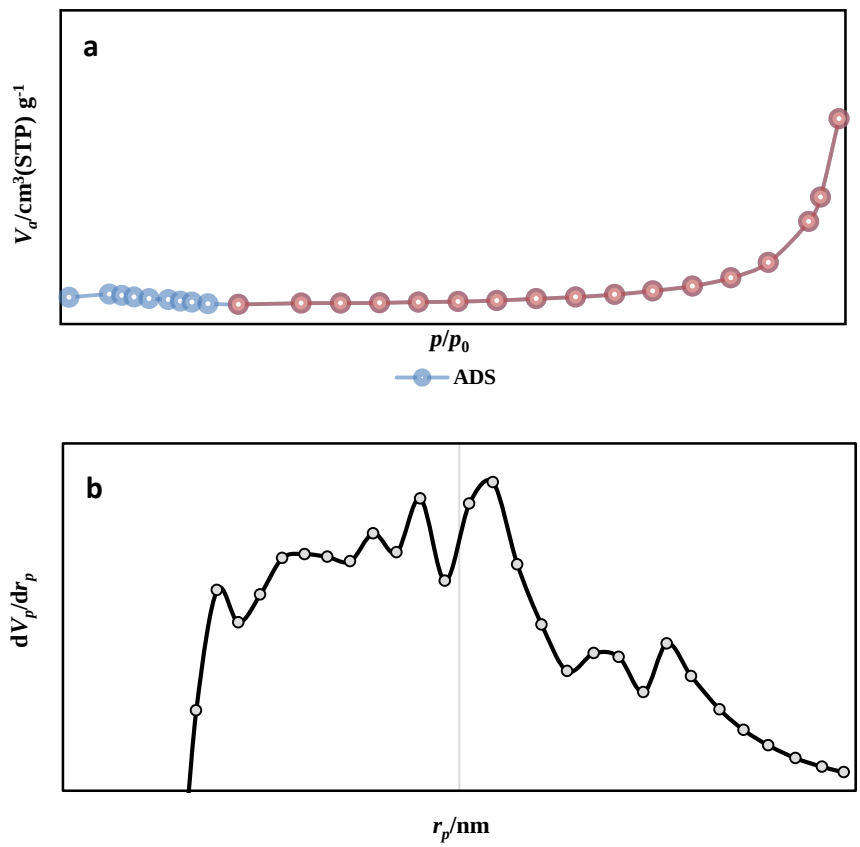

Figure 10: Isotherms of adsorption-desorption (a) and the pore size distribution of prepared new composite of (b).

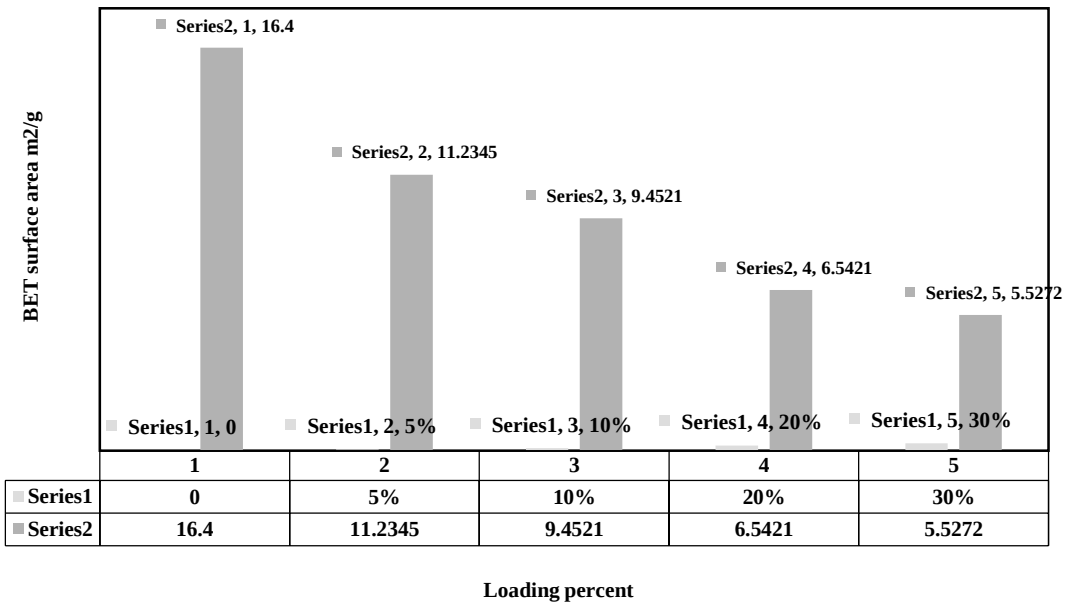

	1	2	3	4	5
Series1	0	5%	10%	20%	30%
Series2	16.4	11.2345	9.4521	6.5421	5.5272

Figure 11: BET surface area of prepared compoites with different loading percent.

3.2. Main effect plot for organic removal

The effect of main on the organic pollutants in RWW as shown in Figure 12, the best set of crucial parameters to combine in order to achieve the desired oxidation performance for $CoWO_4$ /NCW. Every graphic shows which set of limitations works best for a given set of performance indicators. Prior studies have consistently demonstrated an increase in organic elimination at higher adsorbent dosage, pH, temperature, and time levels [29].

The results of independent variables in work shown in Figure 13 show that for all initial organic pollutants values for the new composite, the efficiency of elimination OP rises with time, pH, dose and temperature during adsorption and solar oxidation. Due to insufficient surface area on the oxidation material in these situations, there is a propensity for a fall at a certain point, making it more difficult to obtain a relatively high elimination ratio [30].

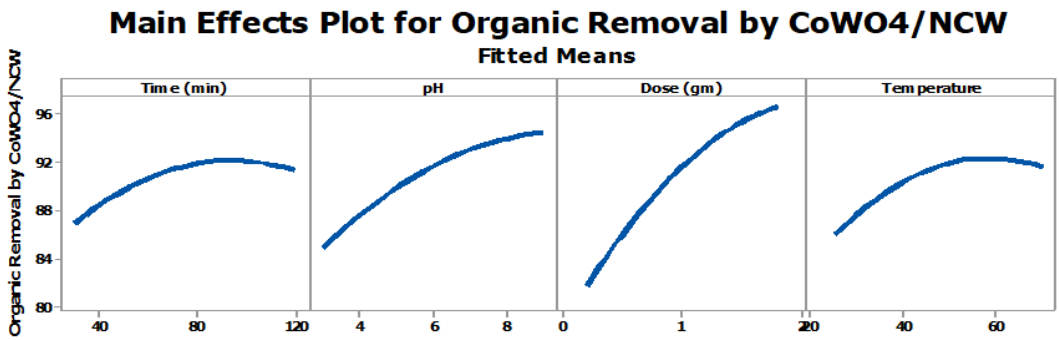

Figure 12: Main effects of organic removal in RWW.

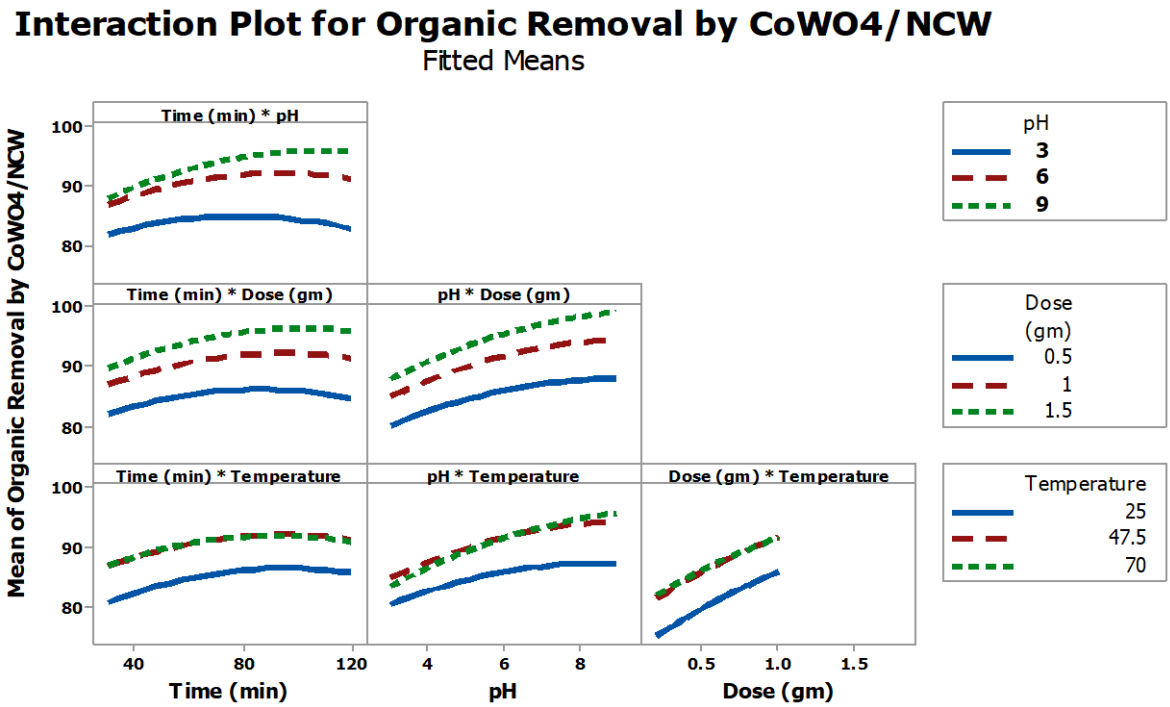

Figure 13: Plot effect of variables of organic removal in RWW.

3.3. Adsorption/ solar degradation treatment

The effect of time on organic elimination from wastewater using nanocomposites involves the kinetics of adsorption and solar degradation processes, optimizing treatment duration. The time required for important degradation of OP depends on factors such as the intensity or duration of solar irradiation, the concentration and type of organic pollutants, and the efficiency of the nanocomposite material in generating reactive species under sunlight [31]. Figure 14a illustrates the link between solar time and organic elimination efficiency along the action process. To determine the optimal time for oxidation effectiveness in the removal of organic materials from wastewater, experiments were conducted. An increase in solar time results in an improvement in elimination efficiency. The results were in line with earlier studies' findings, which presented that lengthening the oxidation period enhanced treatment efficiency, as shown by [32]. By using novel nanocomposites comprised of NCW and cobalt tungstate for adsorption and solar degradation, pH significantly influences the removal of organic materials from RWW. Understanding the pH-dependent mechanisms complicated in both processes is vital for optimizing treatment competence and ensuring the long-term stability and effectiveness of the treatment system. The influence of pH on the adsorption of organic contaminants by adsorbent was investigated across a pH range of 3 to 9, with a contact time of 120 minutes for all experiments.

Figure 14b illustrates that the highest adsorption and photo degradation competences for CW, NaOH/CW, NCW, and $CoWO_4$/NCW were 27.2, 44.2, 70.3, and 81.3 %, respectively, at a pH of 9. These findings align with those reported by Hernández et al. [33]. The experimental observation regarding the use of a basic solution that significant enhancement in OP removal was attained, with the highest elimination experiential at a pH of 9. The dose of nanocomposite material significantly influences organic removal from wastewater through adsorption and solar degradation processes. Optimizing the dose involves balancing removal efficiency, cost considerations, and environmental impact to attain effective and sustainable wastewater treatment [34]. The degradation rate of the OP in RWW under sun irradiation has been used to assess the produced nanocomposite's photocatalytic capability [35]. As the dose increases, Figure 14c shows that organic sorption increases quickly because there are more functional groups available, which opens up more exchangeable surface sites for the formation of complexes with organic content. The exclusion

efficiency has increased for CW, NaOH/CW, NCW, and $CoWO_4$/NCW as the total amount of sorbent that needs to be achieved is increased. (37.2, 45.6, 71.2, and 82.4 percent, in that order). Increased surface area exposed to sunlight may result from higher doses of the prepared composite as solar-catalyst , which could speed up solar breakdown rates. This is so that additional surfaces may be used for photon absorption and the production of reactive species [36]. Generally, increasing temperature can improve adsorption kinetics by facilitating more rapid movement of molecules and increasing the mobility of both adsorbate molecules and active sites on the adsorbent material. Higher temperatures can improve solar degradation processes by increasing the rate of reactions involved [37]. However, excessively high temperatures might also cause degradation of the Nanocomposite material itself, affecting its competence. The beneficial effect of temperature is evident. Increasing the temperature from 25 to 70 °C, the elimination of organic rises from 27.1, 45.2, 71.4, and 80.5 % at 25 to 34.3, 51.8, 76.3, and 87.4 % and at 70 °C for CW, NaOH/CW, NCW, and $CoWO_4$ /NCW respectively as shown in Figure 14d.

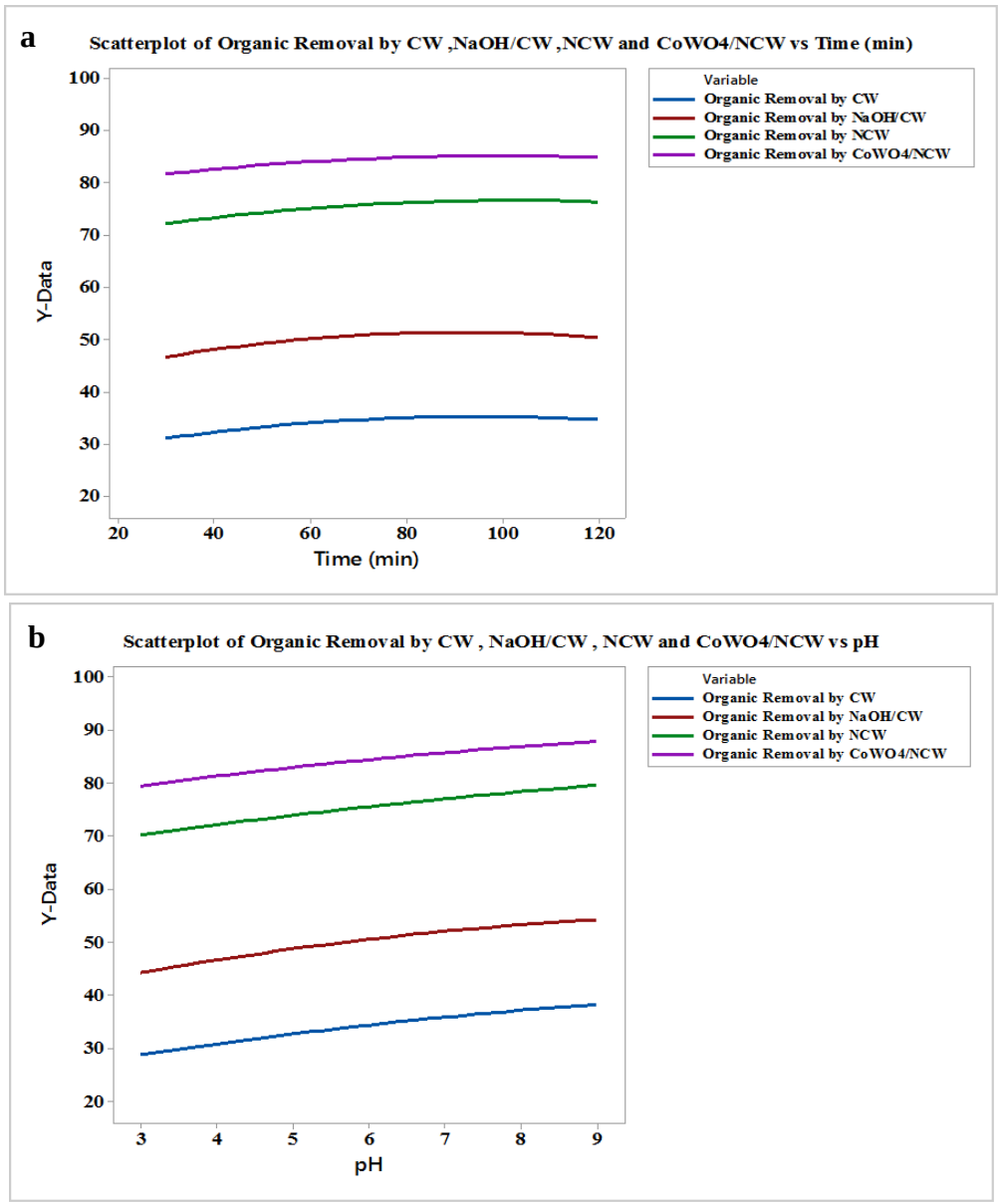

Figure 14: Effect of a) time, b) pH, c) dose, and d) temperature of CW, NaOH/CW, NCW, and $CoWO_4$/NCW on organic elimination.

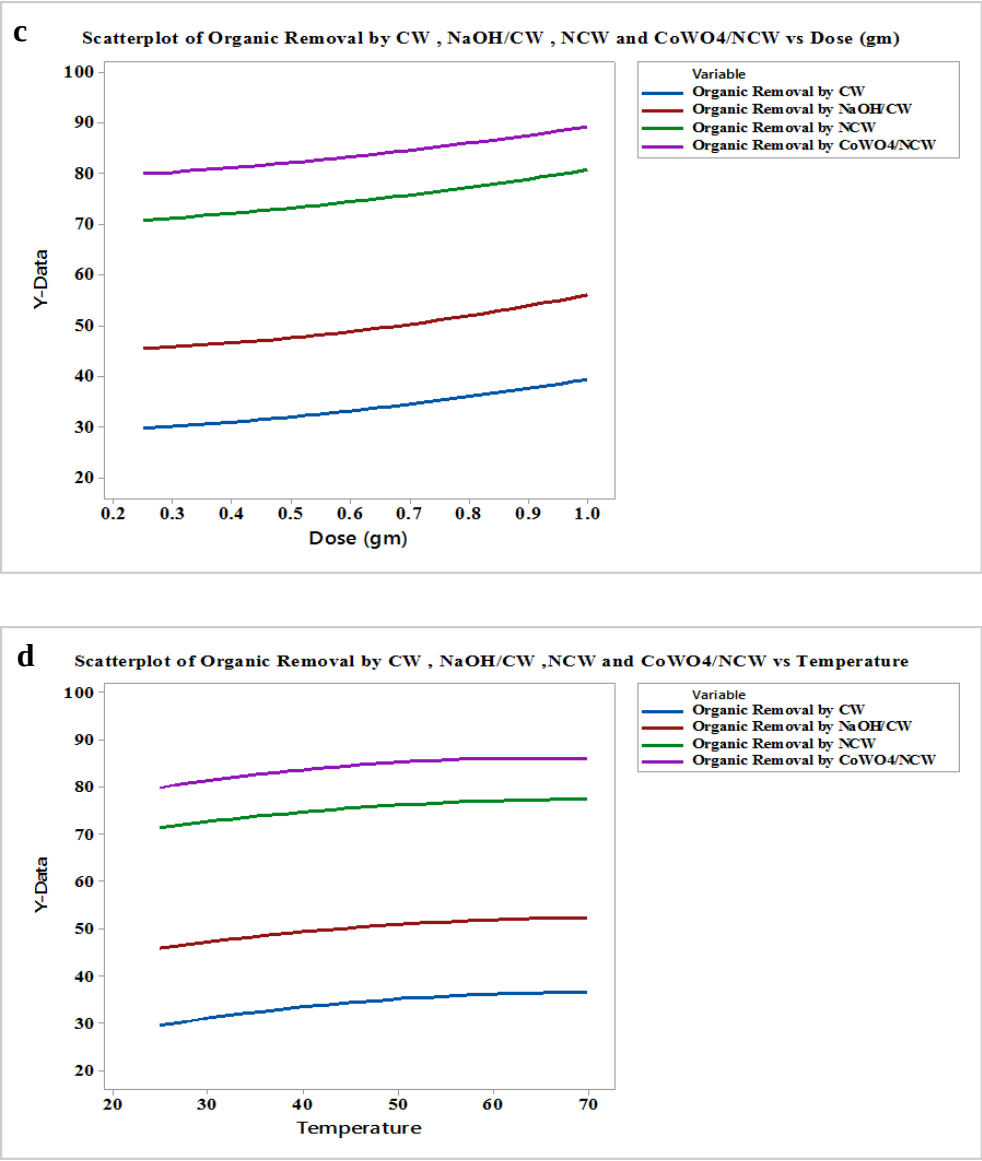

Figure 14: Continue.

3.4. Best of working limits

The best new circumstances for the cotton waste, NaOH/CW, Nano cellulose, and $CoWO_4$/NCW scheme to obtain the best values for working limits for instance dose, pH, oxidation time, and temperature. The measurement implications of the D-optimization are presented in Figure 15. The highest organic elimination competences were 49, 64.2, 90.3, and 97.4 % for CW, NaOH/CW, NCW, and $CoWO_4$ /NCW correspondingly and compared with alike studies in Table 3.

With an emphasis on experimental factors including pollutant type, kind and duration of irradiation, and the accompanying degradation percentages, Table 3 compares the current study with other similar reported works. Notably, when compared to previously report conventional solar-catalysts, the newly synthesized composite solar-catalyst shows excellent performance. This comparison demonstrates the superiority of the synthesized composite photo catalyst over currently available conventional photo catalysts and displays its efficacy and potential in degrading pollutants under diverse experimental circumstances.

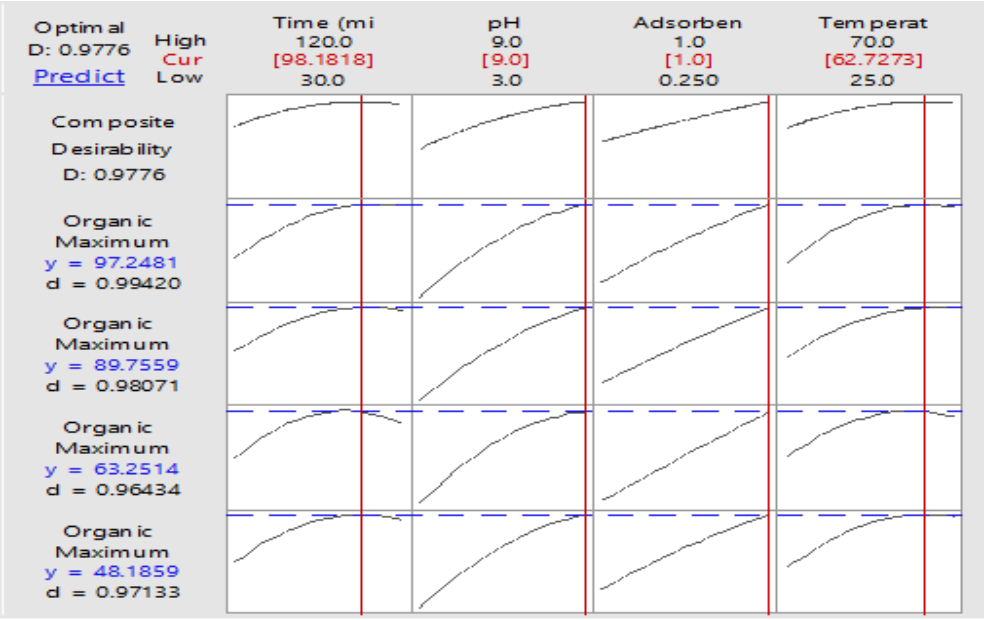

Figure 15: Best working variables on refinery wastewater.

Table 3: Comparison of the current study with other described studies.

Photo-oxidation	Contaminants type	Light type	Time (min)	Degradation (%)	Ref.
TiO_2/Cellulose	Methyl Orange	Solar	30	92	[18]
TiO_2/ Cellulose	Antibacterial	UV	24	91.3	[13]
ZnO/Cellulose Acetate	dyes	UV	20	75	[38]
$CoWO_4$/NCW	OP	Solar	120	97.4	This work

3.5. Oxidation kinetic

The impact of adding cobalt tungstate on organic pollutants solar degradation over NCW. The prepared composite was studied in accordance with certain parameters: change of pH with constants the other parameters with a 0.25 g dose, and a 50 min oxidation. The findings established that as pH rose, more free radicals were produced, which aided in the oxidation of OP and accelerated the reaction. As a result, the degradation rate increased. Though, when the pH level was raised from 7 to 9, there was only a slight increase in organic degradation; it went from 92.1 to 97.4 %. It is difficult to distinguish between different reactions in the complicated processes involved in organic removal from wastewater. Therefore, it is possible to assume estimated kinetics for the organic solution's decomposition. Numerous studies have revealed that the majority of organic elimination curves follow first-order [39]. The model of first order (Eq. 2) is expressed

$$\ln\left[\frac{C_O}{C}\right] = K_1 t \qquad (2)$$

C_o, C_t were in mg/L of the initial organic concentration (both before and after oxidation), time (min) was t and First-order rate constant (min^{-1}) is denoted by K_1.

As shown in Figure 16, the kinetics investigation for the composite adsorbent developed in this work showed a suitable correlation between reaction time and the ratio C_t/C natural logarithm, suggesting a pseudo-first-order kinetic model. When the pH concentration was kept at 9, the prepared composite showed a first-order squalor constant (k_1) value of 0.0674 min^{-1}.

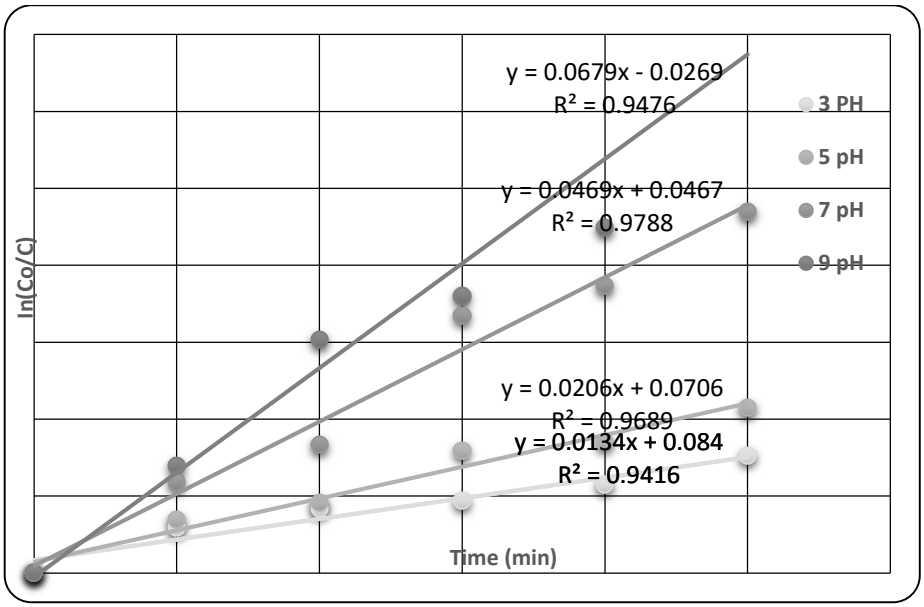

Figure 16: First-order model for solar degradation.

There are various steps in the OP degradation mechanism over the $CoWO_4$/NCW solar catalyst, and certain components of the heterostructure improve. Photoexcitation of the solar-catalyst results in the generation of electron-hole pairs (e_{CB}^- and h_{VB}^+) when it is subjected to visible light with energy equivalent to or greater than its band gap energy in equation 3.

$$CoWO_4/NCW + (\text{solar light}) \rightarrow CoWO_4/NCW\ (e^- + h^+) \quad (3)$$

In the degradation pathway, the interactions between nanoparticles of $CoWO_4$ and NCW are vital. By generating an electric field and altering potentials of band energy, they enable solar produced electrons to move from $CoWO_4$ to NCW and holes to move from NCW to $CoWO_4$. Equation 5 demonstrations the reaction of photo–generated electrons with oxygen molecules (O_{2^-}) to make oxygen radicals (O_{2}•-), while equations 4-6 exemplify the reaction of holes with adsorbed water and hydroxide ions (OH^-) to form free radicals.

$$H_2O + h_{VB}^+ \rightarrow {}^{\bullet}OH + H^+ \quad (4)$$

$$O_2 + e_{CB}^- \rightarrow O_2^{\bullet -} \quad (5)$$

$$O_2^{\bullet -} + H_2O \rightarrow {}^{\bullet}OH + OH^- + O_2 + HO_2^- \quad (6)$$

Furthermore, OP molecules can be directly oxidized by holes. Squalor of the system's organic composition is aided by the manufacture of reactive oxygen species, for example free and oxygen radicals, and direct oxidation by holes. These treatment are graphically depicted in Figure 17, which too shows the migration of electrons and holes, the manufacture of reactive oxygen species, and the resultant organic content degradation across the solar catalyst under visible light irradiation [40]. Table 4 shows the rate constants for the first order of solar-oxidation.

Table 4: pH experimentations.

Sample	$CoWO_4$/NaOH/CW
pH	K_1
3	0.0134
5	0.0206
7	0.0469
9	0.0674

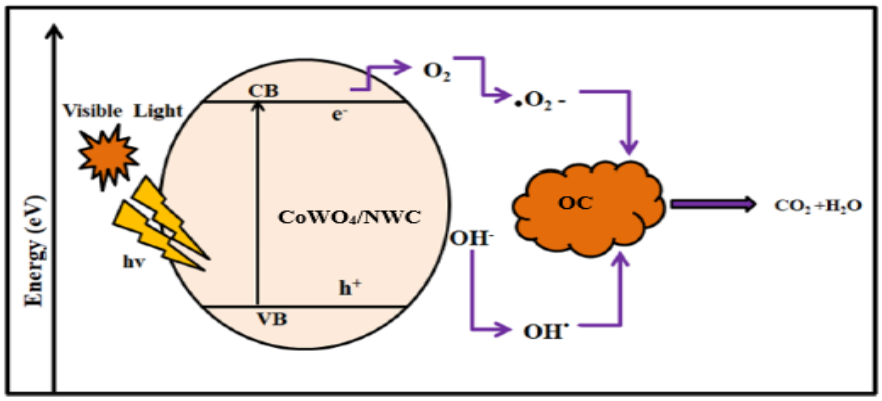

Figure 17: Possible mechanism of solar catalytic degradation.

4. Conclusions

In conclusion, the utilization of a novel composite material derived from cotton waste through acid hydrolysis with nitric acid, combined with cobalt tungstate, presents a promising approach for the removal of OP from RWW. Through adsorption and solar degradation mechanisms, this composite exhibits considerable potential for efficient and sustainable treatment of complex industrial effluents. The cellulose -based composite provides ample surface area and active sites for adsorption, while the incorporation of cobalt tungstate enhances adsorption capacity and selectivity, particularly for specific organic compounds found in refinery wastewater. Solar degradation, facilitated by photocatalytic reactions on the composite surface under sunlight exposure, offers an additional mechanism for organic pollutant removal. The synergy between cellulose-derived components and cobalt tungstate nanoparticles promotes the generation of reactive oxygen species, such as hydroxyl radicals, which efficiently degrade organic contaminants into harmless byproducts. Furthermore, the environmentally friendly nature of the cellulose-derived composite, derived from waste cotton, underscores its potential for sustainable wastewater treatment practices. The utilization of waste materials not only mitigates environmental burdens associated with waste disposal but also offers economic benefits through resource utilization and waste reduction.

5. References

1. Ibrahim HA, Hassan AA, Ali AH, Kareem HM. Organic removal from refinery wastewater by using electro catalytic oxidation. AIP Publishing. 2023; http://dx. doi.org/10.1063/5.0163257.
2. Alturki SF, Suwaed MS, Ghareeb A, AlJaberi FY, Hassan AA. Statistical analysis and optimization of mechanical-chemical electro-fenton for organic contaminant degradation in refinery wastewater. J Eng Res. 2024; http://dx. doi.1063/5.0163257.
3. Naser GF, Dakhil IH, Hasan AA. Organic pollutants removal from oilfield produced water using nano magnetite as adsorbent. Glob NEST J. 2021; 23(3):381-7. http://dx. doi: 10.30955/gnj.003875.
4. Atiyah AS, Al-Samawi AAA, Hassan AA. Photovoltaic cell electro-Fenton oxidation for treatment oily wastewater. AIP Conf Proc. 2020; 2235. http://dx. doi: 10.1063/5.0008937.
5. Ahmed MJ, Mohammed AHAK, Kadhum AAH. Modeling of breakthrough curves for adsorption of propane, n-Butane, and iso-butane mixture on 5A molecular sieve zeolite. Transp Porous Media. 2011; 86(1):215-28. http://dx. doi: 10.1007/s11242-010-9617-5.
6. Kurniawan TW, Sulistyarti H, Rumhayati B, Sabarudin A. Cellulose nanocrystals (CNCs) and cellulose nanofibers (CNFs) as adsorbents of heavy metal ions. J Chem. 2023. http://dx. doi: 10.1155/2023/5037027.
7. Anastopoulos I, Ahmed MJ, Ojukwu VE, Danish M, Stylianou M, Ighalo JO. A comprehensive review on adsorption of Reactive Red 120 dye using various adsorbents. J Mol Liq. 2023; 123719. http://dx. doi.org/10.1016/j.molliq.2023.123719.
8. Vargas AR, García LP, Guillen CS, AlJaberi FY, Salman AD, Alardhi SM, et al. Performance evaluation of a flighted rotary dryer for lateritic ore in concurrent configuration. Heliyon. 2023; 9(11): e21345. http://dx. doi: 10.1016/j.heliyon.2023.e21345.

9. Négrier M, El Ahmar E, Sescousse R, Sauceau M, Budtova T. Upcycling of textile waste into high added value cellulose porous materials, aerogels and cryogels. RSC Sustain. 2023;1(2):335-45. http://dx. doi: 10.1039/d2su00084a.
10. Ahmed MJ, Anastopoulos I, Kalderis D, Haris M, Usman M. Insight into the wheat residues-derived adsorbents for the remediation of organic and inorganic aquatic contaminants: A review. Environ Res. 2024; 118507. http://dx. doi.org/10.1016/j. envres.2024.118507.
11. Kayan GÖ, Kayan A. Composite of Natural Polymers and Their Adsorbent Properties on the Dyes and Heavy Metal Ions. J Polym Environ. 2021; 29(11):3477-96. https://doi.org/10.1007/s10924-021-02154-x.
12. Castañeda Juárez M, Martínez Miranda V, Almazán Sánchez PT, Linares Hernández I, Vázquez Mejía G. Electrosynthesis of sodium and potassium ferrate for the treatment of indigo blue aqueous solutions and denim wastewater. Rev Int Contam Ambient. 2020; 36(3):607-22. http://dx. doi: 10.20937/RICA.53381.
13. Kamel S. Recent development of cellulose/TiO_2 composite in water treatment. Egypt J Chem. 2022; 65(13):601-12. http://dx. doi: 10.21608/ejchem. 2022. 128431.5689.
14. Al-Jubouri SM, Sabbar HA, Lafta HA, Waisi BI. Effect of synthesis parameters on the formation 4a zeolite crystals: Characterization analysis and heavy metals uptake performance study for water treatment. Desalin Water Treat. 2019;165:290-300. http://dx. doi: 10.5004/dwt.2019.24566.
15. Liu J, Chen F, Yao Q, Sun Y, Huang W, Wang R, et al. Application and prospect of graphene and its composites in wastewater treatment. Polish J Environ Stud. 2020; 29(6):3965-74. http://dx. doi: 10.15244/ pjoes/117660.
16. Vosoughifar M. Simple route for preparation cobalt tungstate nanoparticles with different amino acids and its photocatalyst application. J Mater Sci Mater Electron. 2017; 28(11):8011-6. http://dx. doi: 10.1007/ s10854-017-6505-6.
17. Alamery HRD, Hassan AA, Rashid AH. Copper removal in simulated wastewater by solar fenton oxidation. AIP Conf Proc. 2023; 2806(1). http://dx. doi: 10.1063/5.0167259.
18. Jothivenkatachalam K, Prabhu S, Nithya A, Chandra Mohan S, Jeganathan K. Solar, visible and UV light photocatalytic activity of $CoWO_4$ for the decolourization of methyl orange. Desalin Water Treat.2 015;54(11):3134-45. http://dx.doi:10.1080/19443994. 2014.906324.
19. Flihh SM, Ammar SH. Fabrication and photocatalytic degradation activity of core/shell ZIF-67@$CoWO_4$ @CoS heterostructure photocatalysts under visible light. Environ Nanotechnology, Monit Manag. 2021; 16:100595. https://doi.org/10.1016/j.enmm. 2021. 100595.
20. Theivasanthi T, Christma FLA, Joshua A, Gopinath SCB. Synthesis and characterization of cotton fiber-based nanocellulose. Int J Biol Macromol. 2018; 109:832-6. http://dx.doi.org/10.1016/j.ijbiomac. 2017. 11.054.
21. Mondal MS, Paul A, Rhaman M. Recycling of silver nanoparticles from electronic waste via green synthesis and application of AgNPs-chitosan based nanocomposite on textile material. Sci Rep. 2023;13(1):1-15. https://doi.org/10.1038/s41598-023-40668-7.
22. Shekofteh-Gohari M, Habibi-Yangjeh A. Fe_3O_4/ZnO/$CoWO_4$ nanocomposites: Novel magnetically separable visible-light-driven photo-catalysts with enhanced activity in degradation of different dye pollutants. Ceram Int. 2017;43(3):3063-71. http://dx.doi.org/10.1016/j.ceramint.2016.11.115.
23. Hassan AA, Shakir IK. Kinetic Insights into Solar-Assisted Fabrication and Photocatalytic Performance of $CoWO_4$/NCW Heterostructure. Bull Chem React Eng Catal. 2024;10. http://dx. doi.org/10.9767 /bcrec. 20198.
24. Raheem S, Al-yaqoobi A, Znad H, Abid HR. Caffeine extraction from spent coffee grounds by solid-liquid and ultrasound-assisted extraction: Kinetic and thermodynamic study. Iraqi J Chem Pet Eng. 2024; 25(1):49-57. http://dx. doi.org/10.31699/IJCPE. 2024.1.5.
25. Simayee M, Iraji zad A, Esfandiar A. Green synthesize of copper nanoparticles on the cotton fabric as a self-regenerating and high-efficient plasmonic solar evaporator. Sci Rep. 2023;13(1):1-11. https://doi. org/10.1038/s41598-023-40060-5.
26. Alfattal AH, Abbas AS. Synthesized 2nd generation zeolite as an acid-catalyst for esterification reaction. Iraqi J Chem Pet Eng. 2019; 20(3):67-73. http://dx. doi: 10.31699/ijcpe.2019.3.9.
27. Mhawesh TH, Abd Ali ZT. Reuse of brick waste as a cheap-sorbent for the removal of nickel ions from aqueous solutions. Iraqi J Chem Pet Eng. 2020;21(2):15-23.http://dx. doi:10.31699/ijcpe. 2020. 2.3.
28. Pandi N, Sonawane SH, Anand Kishore K. Synthesis of cellulose nanocrystals (CNCs) from cotton using ultrasound-assisted acid hydrolysis. Ultrason Sonochem. 2021; 70:105353. http://dx. doi: 10.1016/j. ultsonch.2020.105353.
29. Nidheesh P V., Gandhimathi R. Textile wastewater treatment by electro-fenton process in batch and continuous modes. J Hazardous Toxic Radioact Waste. 2015; 19(3):04014038. http://dx. doi: 10.1061/ (asce)hz.2153-5515.0000254.
30. Jorgetto AO, Silva RIV, Saeki MJ, Barbosa RC, Martines MAU, Jorge SMA, et al. Cassava root husks powder as green adsorbent for the removal of Cu(II) from natural river water. Appl Surf Sci.2014; 288:356-62. http://dx.doi.org/10.1016/j.apsusc.2013.10.032.
31. Al-Hassan AA, Shakir I. Enhanced Photocatalytic Activity of CuO/NCW via Adsorption Optimization

for refinery wastewater. Iran J Chem Chem Eng. 2024; (Articles in Press). http://dx. doi: 10.30492/ ijcce.2024.2034599.6684.
32. Esteban García AB, Szymański K, Mozia S, Sánchez Pérez JA. Treatment of laundry wastewater by solar photo-Fenton process at pilot plant scale. Environ Sci Pollut Res. 2021; 28(7):8576-84. http://dx. doi: 10.1007/s11356-020-11151-x.
33. Peralta-Hernández JM, Vijay S, Rodríguez-Narváez O, Pacheco-Álvarez MA. Photo and solar fenton processes for wastewater treatment. Electrochem Water Wastewater Treat. 2018; 223-237. http://dx. doi: 10.1016/B978-0-12-813160-2.00009-2.
34. Amdeha E. Biochar-based nanocomposites for industrial wastewater treatment via adsorption and photocatalytic degradation and the parameters affecting these processes. Biomass Convers Biorefinery. 2023;0123456789. https://doi.org/10. 1007/ s13399- 023-04512-2.
35. Ahsan H, Shahid M, Imran M, Mahmood F, Siddique MH, Ali HM, et al. Photocatalysis and adsorption kinetics of azo dyes by nanoparticles of nickel oxide and copper oxide and their nanocomposite in an aqueous medium. Peer J. 2022; 10:1-26. http://dx. doi: 10.7717/peerj.14358.
36. Blachnio M, Zienkiewicz-Strzalka M, Derylo-Marczewska A, Nosach L V., Voronin EF. Chitosan–silica composites for adsorption application in the treatment of water and wastewater from anionic dyes. Int J Mol Sci. 2023;24(14). http://dx.doi:10. 3390/ ijms241411818.
37. El Kaim Billah R, Ayouch I, Abdellaoui Y, Kassab Z, Khan MA, Agunaou M, et al. A novel chitosan/nano-hydroxyapatite composite for the adsorptive removal of Cd(II) from aqueous solution. Polymers (Basel). 2023; 15(6). http://dx. doi: 10.3390/polym15061524.
38. Abu-dalo MA, Al-rosan SA, Albiss BA. Photocatalytic degradation of methylene blue using polymeric membranes based on cellulose acetate impregnated with ZnO nanostructures. Polymers (Basel). 2021;1-17. http://dx.doi.org/10.3390/polym 13193451.
39. Al-jubouri SM, Sabbar HA, Khudhair EM, Ammar SH, Al S, Yas S, et al. Silver oxide-zeolite for removal of an emerging contaminant by simultaneous adsorption-photocatalytic degradation under simulated sunlight irradiation. J Photochem Photobiol A Chem. 2023;442:114763.https://doi.org/10.1016/j.jphotoche m. 2023.114763.
40. Somwanshi SB, Somvanshi SB, Kharat PB. Nanocatalyst: A brief review on synthesis to applications. J Phys Conf Ser. 2020; 1644(1). http://dx. doi: 10.1088/1742-6596/1644/1/012046.

How to cite this article:
Hassan AA, Kareem Shakir I. Fabrication of Solar-Driven new composite Heterostructure $CoWO_4$/NCW Photo catalysts for Enhanced Adsorption /Photo Degradation Activity of organic pollutants. Prog Color Colorants Coat. 2025;18(2):201-218. https://doi.org/10.30509/pccc.2024. 167338.1308.